Photochemical Syn−Anti Isomerization Reaction in 1-Methyl-N^4-hydroxycytosine. An Experimental Matrix Isolation and Theoretical Density Functional Theory Study

Tetyana Stepanenko,[†] Leszek Lapinski,[†] Andrzej L. Sobolewski,[†] Maciej J. Nowak,*[,†] and Borys Kierdaszuk[‡]

Institute of Physics, Polish Academy of Sciences, Al. Lotnikow 32/46, 02-668 Warsaw, Poland, and Department of Biophysics, Institute of Experimental Physics, University of Warsaw, Al. Żwirki i Wigury 93, 02-089 Warsaw, Poland

Received: April 26, 2000; In Final Form: July 10, 2000

The photoreaction converting the syn form of the imino tautomer of 1-methyl-N^4-hydroxycytosine into the anti form was observed for the compound isolated in argon, nitrogen, and xenon low-temperature matrixes. It was found that the reaction is reversible and that it leads to a photostationary point. The assignment of the form initially present in the matrix to the syn isomer and of the photoproduct to the anti isomer was based on the good agreement between the experimental IR spectra and the spectra theoretically simulated at the density functional theory (B3LYP/6-31G**) level.

Introduction

The promutagenic activity of N^4-hydroxycytosine (OH^{4}C) and N^4-methoxycytosine (OMe^{4}C),[1] which are the products of the reaction of the known mutagens hydroxylamine (NH_2OH) and methoxylamine (NH_2OCH_3) with cytosine in RNA and DNA,[2] stems from their ability to base pair like cytosine or like uracil, the last one leading to a C → U(T) transition.[3] This dual functionality of OH^{4}C and OMe^{4}C is due to their existence as an equilibrium mixture of amino and imino tautomers (N^{4}H−N(3)H), and syn and anti rotamers relative to the ring N(3), with the imino-syn form being predominant.[4,5] The methylated analogue 1-methyl-N^4-hydroxycytosine (1-mOH^{4}C), considered in the present work, was found to exist in solution and in crystals predominantly also in the imino form,[4−6] with the exocyclic group in the syn conformation.[7,8] Both tautomeric and conformational equilibria play a key role in base pairing with potentially complementary free bases in solution[9] or in the self-complementary oligonucleotide duplexes.[10−14] These equilibria are of importance for inhibition of thymidylate synthase by 5′-phosphate-N^4-hydroxycytidine, where the syn conformer leads to a 10^4-fold diminution of inhibitory potency.[15]

The formation of Watson−Crick-type pairs with adenine (adenosine) is possible only for the imino-anti isomer of OH^{4}C (or 1-mOH^{4}C) (Chart 1). The syn conformer had a destabilizing effect on the self-complementary oligonucleotide duplexes containing an OH^{4}C−Ade base pair.[10−14]

The structure and the relative energies of OH^{4}C isomers were studied theoretically by Les et al.[16] Their ab initio MP2/6-31G** calculations resulted in the prediction that the syn and anti imino isomers of the compound will be the most stable ones, the syn isomer being lower in energy by 12.8 kJ/mol. The other possible isomers were found to be much higher in energy (by more than 40 kJ/mol) and quite unlikely to be populated. At the same level of theory the energy of the transition state for rotation around the C4═N bond was calculated. This transition state was predicted to be higher in energy by 185 kJ/mol than the syn isomer. Such a high-energy barrier should prevent a spontaneous syn−anti flip at moderate temperatures. It seems very probable that the introduction of the methyl group at N1 does not appreciably change the height of this barrier and that the value calculated by Les et al.[16] is close to that expected for 1-mOH^{4}C studied in the present work.

CHART 1: Possible Structure of the Hydrogen-Bonded Heteroassociate (Watson−Crick Complex) of the Imino-Anti Form of N^4-Hydroxycytosine with Adenosine

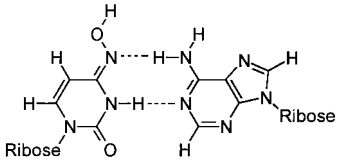

The syn−anti photoisomerization reactions in imines are well-known.[17−19] Though the mechanism of the syn−anti isomerization at the C═N double bond is generally similar to that of the cis−trans photoisomerizations of polyenes,[17] it is more complex. Only the rotation around the C═C double bond is possible for ethylene derivatives, whereas for molecules with the C═N double bond two linearly independent motions—twisting and in-plane inversion (or their combination)—should be considered.[19] Moreover, in the latter case n → π^* excitations have to be considered in addition to $\pi \rightarrow \pi^*$ excitations. The mechanism of syn−anti isomerization via an excited state was proposed by Bonacic-Koutecky and Michl[19] on the basis of the quantum chemical calculations of the potential energy surfaces of the ground state and the lowest excited state of formaldimine. According to this mechanism, the imino group is planar for the ground-state S_0, while in the S_1 and T_1 states the perpendicular geometry should be preferred. Excitation into the S_1 state should be followed by vibrational relaxation to an orthogonally twisted geometry and to the funnel in S_1. After a very rapid radiationless relaxation to S_0, the molecule should relax vibrationally to one of the two planar forms (syn or anti).

As far as oximes are concerned, the syn−anti photoisomerizations in aldoximes have been known since the turn of the

* To whom correspondence should be addressed. E-mail: mjnow@ifpan.edu.pl.
† Polish Academy of Sciences.
‡ University of Warsaw.

10.1021/jp001595n CCC: $19.00 © 2000 American Chemical Society
Published on Web 10/03/2000

CHART 2: Syn and Anti Rotamers of the Imino Form of 1-Methyl-*N*^{4}-hydroxycytosine (1-mOH^{4}C)

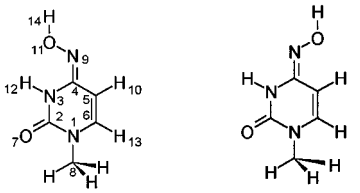

century.[20,21] The syn−anti photoisomerizations reported so far concern compounds in liquid solutions. Analogous reactions for oximes with the C═N double bond attached directly to the ring have not been widely studied, and the reported cases are quite scarce.[22,23] The photoreaction described in the present paper concerns 1-mOH^{4}C—that is, a compound with the C═N group directly attached to the heterocyclic ring. This photoreaction of 1-mOH^{4}C was investigated for isolated molecules frozen in a rigid and inert environment.

Experimental Section

1-mOH^{4}C used in this study was synthesized from 1-methylcytosine and hydroxylamine according to the procedure of Janion and Shugar[24,25] and, independently, from 1-methyluracil by the activation of the 4 position by the triazole moiety.[26] The compound was purified by vacuum sublimation prior to experiment. The structure and purity of the compound were confirmed chromatographically and by ^{1}H and ^{13}C NMR spectra, and by pH-dependent UV absorption spectra.[6] The matrix-isolation infrared spectra of the samples coming from both syntheses were identical in all details. The sample was heated in a microoven placed in the vacuum chamber of the cryostat. The vapors of 1-mOH^{4}C were deposited, together with a large excess of a matrix gas, on a CsI window cooled to 10 K. For UV spectroscopy the matrixes were deposited on a sapphire window. The matrix gases argon, nitrogen, and xenon (all of spectral purity) were supplied by Linde AG, Technische Gase (Berlin), and Norsk Hydro, respectively. The infrared spectra were recorded with a Perkin-Elmer 580B spectrometer at 1−3 cm^{-1} resolution. Integral intensities of the IR absorption bands were measured by numerical integration.

UV absorption spectra were taken using a 480 mm focal length monochromator (Digikroem 480), deuterium lamp, and Philips XP2020 photomultiplier. The signal was registered in the single photon counting mode.

Matrixes were irradiated with light from the high-pressure mercury lamp, HBO 200, fitted with a water filter and a cutoff filter, WG 295, transmitting light with $\lambda > 295$ nm. In some experiments the matrixes were additionally irradiated with a lamp fitted with a WG 335 filter.

Computational Section

The ground-state geometries of the syn and anti isomers of 1-mOH^{4}C were optimized using the density functional theory (DFT) combined with Becke's three-parameter exchange functional and the gradient-corrected functional of Lee, Yang, and Parr DFT(B3LYP).[27] The standard 6-31G** basis set was used in these calculations. Harmonic vibrational frequencies and absolute IR intensities were calculated at the optimized geometries. These calculations were carried out for the structures presented in Chart 2. The structures which differ from those presented in the chart by a rotation of the methyl group were found to be higher in energy. The computed frequencies were scaled by a single factor of 0.98 to approximately correct for vibrational anharmonicity, basis set truncation, and partial neglect of electron correlation. The standard PED analysis[28] of the calculated normal modes has been done. Internal coordinates used in this analysis are analogous to those previously defined for uracil and cytosine.[29−31] The PED matrix elements greater than 10% are listed in Tables 1 and 2.

For the construction of the reaction path for isomerization, the coordinate-driven minimum-energy path (MEP) was adopted; i.e., for a given value of the torsion around the C═N bond, all remaining intramolecular coordinates were optimized. The ground-state reaction-path calculations were performed at the restricted Hartree−Fock (RHF) level, while for the excited-state optimizations the configuration interaction method with single excitations from the RHF reference (CIS) was utilized. All calculations were performed with the Gaussian 94 program.[32]

Results and Discussion

A part of the infrared spectrum of 1-mOH^{4}C isolated in an Ar matrix is presented in Figure 1b. The infrared spectrum changes after irradiation of the matrix with the high-pressure mercury lamp fitted with the WG 295 cutoff filter (Figure 1c); i.e., the initial spectrum decreases and a new spectrum appears. The spectra of the substrate and of the photoproduct were identified as due to the syn and anti isomers of the compound (see further discussion below). Even after prolonged (several hours) irradiation, it was not possible to completely transform the initial syn form of the compound into the anti isomer. The rate of the reaction (upon conditions described above) was quite fast initially, but then the reaction reached a photostationary point, which did not change any further with time (Figure 2). This photostationary point corresponds to the transformation of about 60% of the initial form into the photoproduct. The fact that a photostationary state is set up indicates that reactions in both directions (syn → anti and anti → syn) occur simultaneously in the UV-irradiated sample. The reverse reaction was observed directly when the matrix was additionally irradiated with the same Hg lamp but fitted with the WG 335 filter (Figure 1a). The anti form created during the previous irradiation (with the WG 295 filter) mostly disappears, and the population of the initial syn isomer rebuilds.

The UV absorption spectra of 1-mOH^{4}C isolated in Ar and N_2 were recorded just after the deposition of the matrixes and after UV (WG 295) irradiation of the samples (Figure 3). The diffuse shape of the spectra at longer wavelengths and the lack of a well-defined long-wavelength edge are typical characteristics of a system with a C═C or a C═N bond capable of cis−trans or syn−anti isomerization around the double bond. In such systems, due to the very different shapes of the ground- and excited-state potential energy surfaces, the intensity pattern is governed by the Franck−Condon factors, which are very small for the 0−0 transition. This transition is therefore usually not observed, and there is no sharp long-wavelength edge of the spectrum. On inspecting the spectra presented in Figure 3, it is clear that at $\lambda > 300$ nm the photoproduct absorbs stronger than the initial form. Therefore, irradiation with long-wavelength light should promote excitations and photochemical transformation of the anti form initially not present in the matrix.

The observations described above clearly indicate that the photoreaction in question is reversible and that the final stage of the reaction is always a photostationary point. The position of this photostationary point depends on the wavelengths of the light inducing the reaction. The matrix environment can also

TABLE 1: Experimental and Calculated IR Spectra of the Syn Form of 1-Methyl-N^4-hydroxycytosine[a]

experimental		Ar matrix	N_2 matrix		calculated DFT(B3LYP)/6-31G**		
$\tilde{\nu}$, cm^{-1}		I, rel.	$\tilde{\nu}$, cm^{-1}	I, rel.	$\tilde{\nu}$, cm^{-1}	A^{th}, km/mol	PED (%)
3648		155	3635	206	3768	119	νOH(100).
3445		105	3432	135	3567	70	νNH(100).
2982			2997		3197	1	νC5H10(96).
2977			2972		3156	4	νC6H13(96).
2956		41	2958	30	3126	0.2	ν_2Me(91).
2944			2940		3045	26	ν_3Me(100).
2937					2986	70	ν_1Me(91).
1847		10	1802	4			
1772		3	1785	6			
1739			1739		1774	585	νCO(76).
1724		639	1724	647			
1684		328	1690 sh		1702	246	νC5C6(30), νC4N9(30).
1681			1678	286			
1622		4	1621	3	1644	4	νC4N9(39), νC5C6(34).
			1598	4			
1592		1	1594				
1520							
1507							
1485			1486		1492	62	β_2Me(73), β_3Me(12).
1475		50		43	1488	9	β_4Me(93).
1468			1469		1472	37	νC4C5(25), νC6N1(19), βC6H13(15).
			1435	9			
1423		14	1415	9	1428	18	β_1Me(62), βN3H12(9).
1407		23	1392	39	1415	33	βN3H12(35), βOH(12), β_1Me(10).
1385		68	1380	56	1381	58	βC6H13(17), νN1C2(14), β_1Me(15),
1362 sh							βC5H10(11).
			1330				
1322		34	1324	43	1318	41	νC6N1(18), β_3Me(16).
1285		155	1290	135	1283	199	βOH(53), νC2N3(14), βC6H13(10).
1274 sh			1277 sh				
1264		27	1270	78	1262	49	βN3H12(19), νN3C4(15), νC2N3(14),
							βC6H13(13), βC5H10(11), βOH(10).
1226		5			1192	8	νN1C8(47), νC2N3(19), β_1R(15).
1155		14	1153	11	1157	19	βC5H10(36), β_3Me(24), βC6H13(22).
1136		1					
					1136	0.3	β_5Me(92).
1034							
1026		23	1036	35	1021	14	β_3Me(37), νC6N1(20), βC5H10(12).
987		6	986	4	981	33	β_1R(18), νC4C5(17), νN3C4(16), νN1C2(11).
949 sh							
940 sh			944 sh				
927		151	932	121	946	198	νNO(78).
916			924 sh				
					928	0.3	γC6H13(79), γC5H10(39).
					800	0.3	β_1R(41), νN1C8(17).
761		5	765	4	762	19	γC5H10(59), γC6H13(25), γC4N9(12).
					738	3	νN1C2(34), νN1C8(15), νC6N1(11).
747		68	751	74	726	54	γCO(96).
					664	5	γC4N9(60), τ_1R(26).
614		64	641	43	632	60	γN3H12(98).
604 sh							
					598	2	β_3R(36), νC5C6(16), νC4C5(11), βN1C8(10).
580		18	579	26	573	19	βNO(34), β_3R(26), β_2R(11).
572 sh							
					522	1	βCO(44), νC2N3(11), νN3C4(10).
					457	0.2	τNO(28), τ_1R(22), τ_2R(22), τ_3R(21).
399		32	399	43	392	33	β_2R(59), βCO(11).
344		2	340	4	341	3	βN1C8(70).
307		78	379	9	299	138	τOH(73), τ_3R(13).
			361 sh				
					255	15	τNO(41), τOH(19), τ_3R(19), τN1C8(14).
					209	1	β_4Me(55), τ_3R(26).
					193	2	γN1C8(69), τNO(17).
					150	0.3	τ_2R(54), τ_1R(49).
					88	1	τ_3R(56), τ_2R(27), τMe(14).
					64	0.05	τMe(80), γN1C8(22).

[a] I, integral absorbances normalized in such a way that the sum of intensities of all assigned bands is equal to the sum of intensities of the corresponding calculated bands; A^{th}, calculated intensities; sh, shoulder. Internal coordinates used in PED analysis are defined as in refs 29−31. PEDs lower than 10% are not included. Theoretical band positions are scaled by a factor of 0.98.

TABLE 2: Experimental and Calculated IR Spectra of the Anti Form of 1-Methyl-N^4-hydroxycytosine[a]

experimental		Ar matrix	N_2 matrix		calculated DFT(B3LYP)/6-31G**		
$\tilde{\nu}$, cm^{-1}		I, rel	$\tilde{\nu}$, cm^{-1}	I, rel	$\tilde{\nu}$, cm^{-1}	A^{th}, km/mol	PED (%)
3648		155	3634	148	3757	94	νOH(93).
3445		90	3438	103	3562	58	νNH(100).
					3217	5	νC5H10(98).
					3149	6	νC6H13(98).
					3126	0.3	ν_2Me(91).
					3047	25	ν_3Me(100).
					2987	68	ν_1Me(91).
1782		7	1783	4			
1740	}	734	1739	}			
1728	}		1726	} 763	1775	640	νCO(74).
1718	sh		1712	sh			
1694	sh		1691	sh			
1684	sh		1684	sh			
1677		258	1675	359	1704	283	νC4N9(38), νC5C6(22).
					1647	12	νC5C6(39), νC4N9(30), βC6H13(10).
			1541	5			
1497	}	47	1505	}	{ 1492	56	β_2Me(75), β_3Me(12).
1483	}		1484	} 45	{ 1488	9	β_4Me(93).
1455		20	1457	9	1453	34	νN3C4(21), νC4C5(13), βNH(11).
1439		30	1444	31	1437	27	β_1Me(32), βNH(11), βC5H10(11), βOH(10).
1407		25	1412	21	1410	6	β_1Me(50), βC6H13(12).
			1389	sh			
1373		93	1374	74	1367	127	νC2N3(21), νN1C2(15), βNH(14).
1350		4	1352	2			
1333	}	99	1336	81	1332	122	νC6N1(22), βC6H13(13), β_3Me(12).
1327	sh }		1332				
1320	sh }						
1307		30	1315	25	1306	51	βOH(53), βNH(16).
1277		109	1281	}	1268	89	νC2N3(20), νN3C4(15), βC6H13(14), βNH(13).
			1276	} 68			
1205			1218	14	1193	9	νN1C8(49), βOH(16), νC2N3(13).
1160		10	1153	7	1161	8	βC5H10(36), βC6H13(22), β_3Me(23).
					1136	0.3	β_5Me(92).
1052		5					
1031		69	1034	53	1025	42	β_3Me(35), νC6N1(18).
981	}	79	980	52	981	139	νNO(33), νN3C4(17), νC4C5(12), βC4N9(10).
978	}						
			944	sh			
936		119	933	94	940	97	γC6H13(82), γC5H10(37).
925	sh						
					939	0.2	νNO(36), β_1R(16).
790		3	795	4	780	5	νC4C5(29), β_1R(29).
767		20	772	18	777	23	γC5H10(63), γC6H13(23), γC4N9(16).
754		10			744	6	νN1C8(27), νN1C2(25).
749		59	752	54	723	48	γCO(102).
					663	0.01	γC4N9(48), τ_1R(41), τ_2R(12).
					642	4	βNO(31), βCO(22), νN1C2(10).
598		9	598	14	592	7	β_3R(64).
585		60	613	58	611	78	γNH(103).
459		20	463	23	446	24	β_2R(36), βCO(28), βNO(12).
407		9	408	14	394	9	β_2R(32), νC2N3(14), βNO(13), βCO(10), νN3C4(10).
					384	0.01	τ_3R(36), γC4N9(21), τ_1R(19), τ_2R(18).
346		9	343	2	345	7	βN1C8(70).
315		50	379	40	322	78	τNO(36), τOH(51).
256		44			240	59	τNO(42), τOH(40).
					208	0.1	β_5Me(44), τ_3R(31), βC4N9(13).
					206	0.6	γN1C8(80), τ_2R(12).
					135	2	τ_2R(71), τ_1R(40).
					83	0.02	τ_3R(72), τMe(14).
					55	0.01	τMe(80), γN1C8(20).

[a] I, integral absorbances normalized in such a way that the sum of intensities of all assigned bands is equal to the sum of intensities of the corresponding calculated bands; A^{th}, calculated intensities; sh, shoulder. Internal coordinates used in PED analysis are defined as in refs 29−31. PEDs lower than 10% are not included. Theoretical band positions are scaled by a factor of 0.98.

influence the substrate to product ratio after prolonged irradiation of the sample. While for 1-mOH^{4}C isolated in an Ar matrix 60% of the syn form can be converted into the anti isomer (by irradiation through the WG 295 filter), for the compound isolated in a N_2 matrix a stationary state, corresponding to the transformation of 80% of the initial form, occurs already after 30−

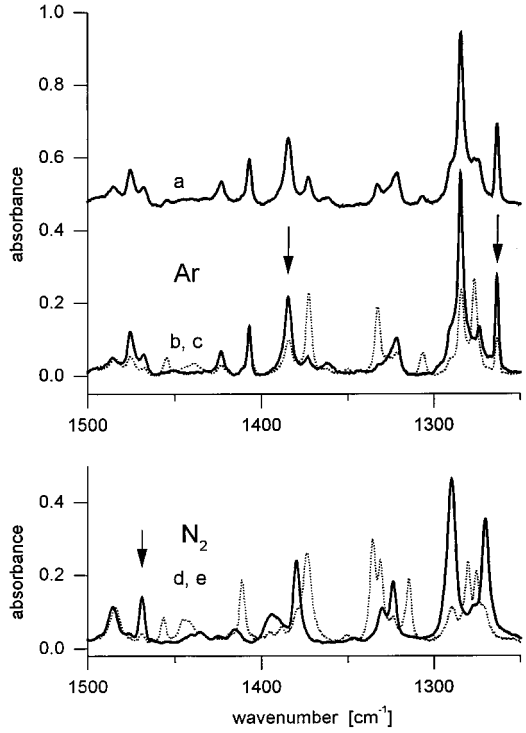

Figure 1. Fragment of the infrared spectrum of 1-mOH^{4}C isolated in an Ar matrix (traces a, b, and c) and in a N_2 matrix (traces d and e), after deposition of the matrix (solid lines b and d), after prolonged UV irradiation through the WG295 filter (dotted lines c and e), and after further irradiation through the WG335 filter (trace a). Arrows point to the bands in the initial spectrum which do not overlap with the spectrum of the photoproduct; the ratio of intensities of these bands before and after prolonged UV (WG295) irradiation illustrates the position of the photostationary state.

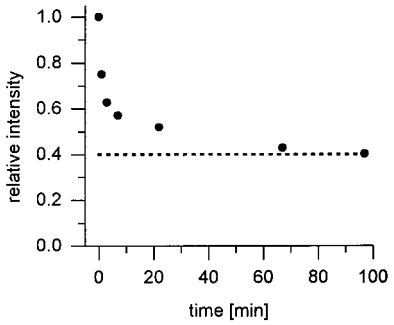

Figure 2. Progress of the syn−anti photoreaction of 1-mOH^{4}C (isolated in an Ar matrix) as a function of the time of UV (WG 295) irradiation. The progress was monitored as a decrease of the intensity of the band at 1385 cm^{-1} with respect to its initial intensity.

40 min of such irradiation (Figure 1d,e). In the case of Xe as the matrix material, however, only a relatively small quantity (about 32%) of the substrate can be converted into the product until the reaction reaches the photostationary point. The reason for these matrix environment effects is not clear. Weak host−guest interactions can lead to slight deformations of the potential energy surfaces in S_1 and S_0 states, which can result in substantial shifts in the photostationary ratio due to the dependence of the photostationary state position upon such changes. We cannot exclude, however, the heavy atom effect promoting intersystem crossing processes.

The comparison of the experimental and the theoretical spectra allows an assignment of the syn and anti structures of the imino−oxo tautomer of 1-mOH^{4}C to the form initially present in the matrix and to the photoproduct, respectively. The

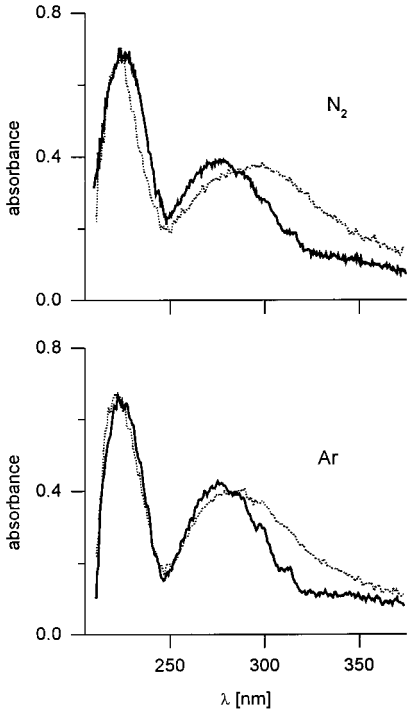

Figure 3. UV absorption spectra of 1-mOH^{4}C isolated in Ar and N_2 matrixes: after deposition, solid lines; after prolonged UV (WG 295) irradiation of the matrixes, dotted lines.

theoretical and experimental spectra are presented in Figure 4. The calculated and experimentally measured positions of the infrared absorption bands, as well as the corresponding intensities, are collected in Tables 1 and 2. The good overall agreement between the theoretical spectrum of the syn isomer and the experimental spectrum of the form initially present in the matrix as well as that of the theoretical spectrum of the anti isomer and the experimental spectrum of the photoproduct leaves practically no doubt about the correctness of the assignment. A detailed consideration of particular fragments of the spectra provides further evidence in favor of this conclusion. Usually, theoretical spectra predicted within the harmonic approximation best reproduce experimental observations in the low-frequency region. Because of the lower density of vibrational states, the anharmonic effects such as Fermi resonances and the bands due to overtones are much less probable in this spectral range. Indeed, the agreement between the theoretical prediction and experiment is particularly good in the region below 1000 cm^{-1}. One band due to OH torsional vibration (τ(OH)) is present in the calculated spectrum of the syn form. Two bands corresponding to normal modes due to the coupled τ(OH) and τ(NO) vibrations are predicted for the anti form. This is in good agreement with the experimental observation of just one band at 307 cm^{-1} (Ar) in the initial spectrum and two bands at 315 and 256 cm^{-1} (Ar) in the spectrum of the photoproduct. These bands are readily identified as due to τ(OH) vibrations, because they change their positions considerably toward higher wavenumbers in the spectrum of 1-mOH^{4}C isolated in the more interacting N_2 matrix. This effect of the matrix environment is a typical characteristic of bands due to τ(OH) vibrations; it has previously been observed for a number of molecules.[33,34]

In the spectrum of the syn isomer the band due to the OH bending vibration (β(OH)) was predicted to be quite strong, much stronger than any other band in the 1400−1200 cm^{-1} region. The opposite was predicted for the anti isomer; no strong

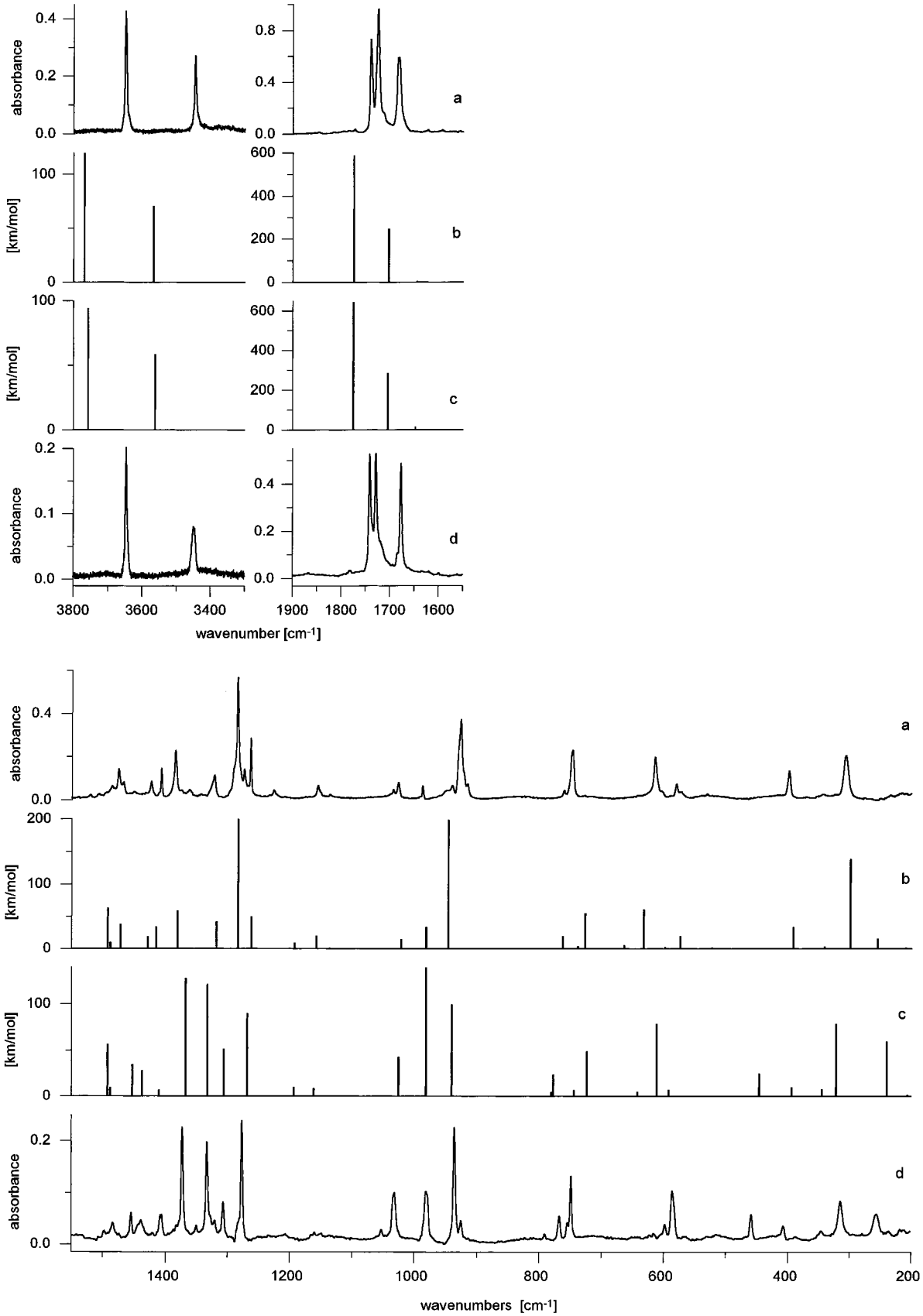

Figure 4. Infrared spectra of 1-mOH[4]C: (a) experimental spectrum of the isomer initially present in the Ar matrix; (b) spectrum of the syn form theoretically calculated at the DFT(B3LYP)/6-31G** level; (c) theoretical spectrum of the anti isomer calculated at the same level; (d) experimental spectrum of the photoproduct. Theoretically calculated wavenumbers were scaled by a single scale factor of 0.98. The spectrum of the photoproduct was obtained by subtracting the initial spectrum (multiplied by 0.4) from the spectrum recorded after UV (WG 295) irradiation of the matrix.

band due to β(OH) should be expected in the IR spectrum of this form. In the initial experimental spectrum a band much stronger than any other in this region was observed at 1285 cm^{-1} (Ar)—a position quite close to the 1283 cm^{-1} theoretically predicted for the β(OH) band in the syn form. This observation supports the assignment proposed above. Moreover, for both

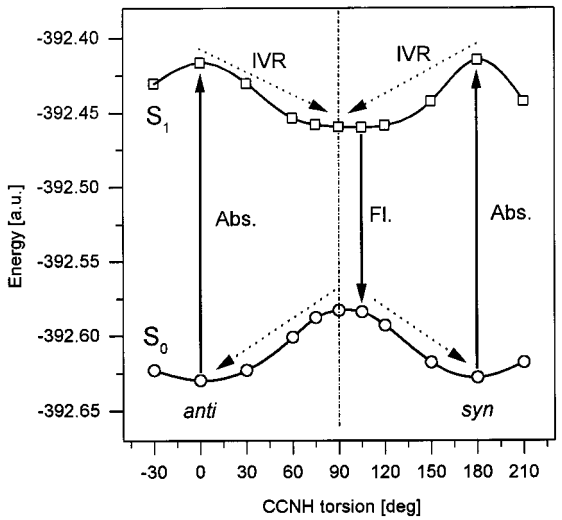

Figure 5. RHF (circles) and CIS (squares) PE profiles of the S_0 and S_1 states of iminocytosine, respectively, calculated along the reaction coordinate for twisting of the C═N bond. The solid arrows indicate vertical absorption (Abs) and fluorescence (Fl) from the minima of the S_0 and S_1 states. The dashed arrows denote vibrational relaxation (IVR) on the PE surface of a given electronic state.

isomers, the experimental and theoretical patterns in the 1400−1200 cm^{-1} spectral range agree with each other very well (see Figure 4).

The 1750−1600 cm^{-1} spectral region carries much less information in that respect. For both isomers two strong bands are predicted: one due to the stretching vibration of the C═O group (ν(C═O)) and the other due to a coupled stretching vibration of the C5C6 and C4N9 double bonds, bands that are clearly observed in the experimental spectra. Both theoretical predictions for this region and the respective experimental observations are very similar for syn and anti forms of 1-mOH^{4}C; hence, no differentiation of the isomers can be made on that basis.

The bands due to the stretching vibration of the OH group were found for the syn and anti isomers at the same spectral position, 3648 cm^{-1}. The same is true for the bands due to the ν(NH) vibration which appear at 3445 cm^{-1} for both isomers (see Figure 4). This overlap, especially that of the ν(NH) bands, shows that there is no NH···O intramolecular hydrogen bond in the syn form of the compound. The hydrogen-bond-like interaction between the oxygen atom from the oxime group and the hydrogen attached to the N3 atom in the ring must be very weak. This is most probably due to the low electron density of the oxygen lone pairs at the position of the hydrogen atom. The latter results from the hybridization of the oxygen atom, which brings the majority of the lone pair density out of the plane of the molecule.

Theoretical Model

To shed some light on the mechanism of the syn−anti isomerizations in iminocytosines, theoretical calculations of the potential energy surface in the S_0 and S_1 states have been performed for a model system, namely, iminocytosine. The minimum-energy-path potential-energy (PE) profiles of the ground state and the lowest excited singlet state of iminocytosine are shown in Figure 5 as a function of the C5−C4−N9−H torsion. A mechanistic model of the photoisomerization reaction is also indicated in the figure. The ground-state PE function of iminocytosine possesses two well-defined local minima corresponding to planar syn and anti conformations of the CHN group, with the latter form being more stable than the former by about 7.1 kJ/mol at the RHF level of theory. This is in qualitative agreement with experimental observations.[35] The two isomers are separated by a sizable barrier for the perpendicular conformation of the NH group. The PE profile of the S_1 state differs remarkably from that of the ground state and shows a single shallow minimum around the perpendicular orientation of the NH group, but it is slightly shifted in the direction of the syn conformation.

The mechanistic picture of the anti−syn photoisomerization resulting from our calculations is as follows. After vertical excitation of either anti or syn isomeric forms of iminocytosine to the S_1 state, vibrational relaxation leads to the orthogonally twisted geometry. Vertical fluorescence from this structure leads the system to a geometry of the ground state, in which the NH group is slightly directed to the syn form. Vibrational relaxation of this structure along the ground-state PE surface is expected to lead to the syn form with higher probability than to the anti form. Since both syn and anti forms are excited to the S_1 state with approximately equal rates, the asymmetry of the S_1 PE profile is thus responsible for the distribution between the reactant and product at the photostationary point. In the case of iminocytosine the above model predicts phototransformation of the anti form into the syn isomer, which is in agreement with experimental observation.[35]

Unlike in the model system formaldimine,[19] our study of iminocytosine does not identify any low-lying conical intersections between the S_0 and S_1 states. One cannot, however, exclude the role of intersystem crossing to the nearby triplets in the course of the photoreaction. Our UHF-DFT(B3LYP) calculation on the T_1 state yields an essentially flat PE profile (free rotation of the NH group) without apparent preference for either of the two isomeric forms (see Figure 6 in the Supporting Information). Such a profile should allow for a second channel (through the T_1 state), leading to a different photostationary ratio. The heavy atom effect may manifest itself by the change of relative probabilities of the two reaction channels.

Conclusions

1-mOH^{4}C, isolated in low-temperature inert gas matrixes, was found to be in the syn form of the imino−oxo tautomer. Upon irradiation of this compound with UV light, the syn form was transformed into the anti isomer. This photoreaction is reversible, its direction depends on the wavelength of UV light, and it ends with a photostationary state. Similar photoinduced syn−anti (or anti−syn) isomerization reactions have also been found for several N^4-hydroxycytosines substituted with methyl groups at different positions.[36]

Relevant to the foregoing is the fact that the mutagenic properties of hydroxylamine are associated with its ability to modify cytosine and adenine residues in DNA to promutagenic analogues, i.e., N^4-hydroxycytosine and N^6-hydroxyadenine, respectively. The conformation of the exocyclic *N*-hydroxyl group is crucial for hydrogen-bonded planar complexes formed between both analogues and potentially complementary bases. In the case of OH^{4}Cyt, a natural Watson−Crick planar complex with adenine is formed only by the imino-anti form, and a wobble base pair is formed with the imino-syn form. In this context, the photochemical syn−anti isomerization of the imino−oxo tautomer of 1-mOH^{4}C, presented in this paper, suggests that similar processes may occur for OH^4-Cyt in nucleic acids.

Acknowledgment. We are obliged to Dr. Z. Kisiel for reading the manuscript and for helpful comments. B.K. thanks

the State Committee for Scientific Research (KBN, Grant Nos. BW-1452/BF and BST-622/BF) and Howard Hughes Medical Institute for an International Research Scholar's award (Grant No. HHMI 75195-543401).

Supporting Information Available: Figure 6 showing the UHF-DFT(B3LYP) potential energy profiles of the S_0 and T_1 states of iminocytosine calculated along the reaction coordinate for twisting of the C═N bond. This material is available free of charge via the Internet at http://pubs.acs.org.

References and Notes

(1) Marfey, P.; Robinson, E. *Mutat. Res.* **1981**, *86*, 155.
(2) Singer, B.; Kusmierek, J. T. *Annu. Rev. Biochem.* **1982**, *52*, 655.
(3) Pavlov, Y. I.; Suslov, V. V.; Shcherbakova, P. V.; Kunkel, T. A.; Ono, A.; Matsuda, A.; Schaaper, R. M. *Mutat. Res.* **1996**, *357*, 1 and references therein.
(4) Kierdaszuk, B.; Shugar, D. *Biophys. Chem.* **1983**, *17*, 285.
(5) Kierdaszuk, B.; Stolarski, R.; Shugar, D. *Eur. J. Biochem.* **1983**, *130*, 559.
(6) Niedzwiecka-Kornas, A.; Kierdaszuk, B.; Stolarski, R.; Shugar, D. *Biophys. Chem.* **1998**, *71*, 87.
(7) Birnbaum, G. I.; Kulikowski, T.; Shugar, D. *Can. J. Biochem.* **1979**, *57*, 308.
(8) Shugar, D.; Huber, C. P.; Birnbaum, G. I. *Biochim. Biophys. Acta* **1976**, *447*, 274.
(9) Shugar, D.; Kierdaszuk, B. *J. Biosci.* **1985**, *8*, 657.
(10) Nedderman, A.; Stone, M.; Williams, D.; Lin, P.; Brown, D. M. *J. Mol. Biol.* **1993**, *230*, 1068.
(11) Stone, M.; Nedderman, A.; Williams, D.; Lin, P.; Brown, D. M. *J. Mol. Biol.* **1991**, *222*, 711.
(12) Fazakerly, G. V.; Gdaniec, Z.; Sowers, L. C. *J. Mol. Biol.* **1993**, *230*, 6.
(13) Gdaniec, Z.; Ban, B.; Sowers, L. C.; Fazakerly, G. V. *Eur. J. Biochem.* **1996**, *242*, 271.
(14) Van Meervelt, L.; Moore, M. H.; Kong Thoo Lin, P.; Brown, D. M.; Kennard, O. *Nucleosides Nucleotides* **1990**, *9*, 467.
(15) Rode, W.; Zieliñski, Z.; Dzik, J. M.; Kulikowski, T.; Bretner, M.; Kierdaszuk, B.; Ciesla, J.; Shugar, D. *Biochemistry* **1990**, *29*, 10835.
(16) Les, A.; Adamowicz, L.; Rode, W. *Biochim. Biophys. Acta* **1993**, *1173*, 39.
(17) Klessinger, M.; Michl, J. *Excited States and Photochemistry of Organic Molecules*; VCH Publishers: New York, 1995; Chapter 7.
(18) Paetzold, R.; Reichenbacher, M.; Appenroth, K. *Z. Chem.* **1981**, *21*, 421.
(19) Bonacic-Koutecky, V.; Michl, J. *Theor. Chim. Acta* **1985**, *68*, 45.
(20) Padwa, A. *Chem. Rev.* **1977**, *77*, 37.
(21) Pratt, A. C. *Chem. Soc. Rev.* **1977**, *6*, 63.
(22) Yates, P.; Wong, J.; McLean, S. *Tetrahedron* **1981**, *37*, 3357.
(23) Suginome, H.; Ohshima, K.; Ohue, Y.; Ohki, T.; Senboku, H. *J. Chem. Soc., Perkin Trans. 1* **1994**, 3239.
(24) Janion, C.; Shugar, D. *Acta Biochim. Pol.* **1965**, *12*, 337.
(25) Brown, D. M.; Hewlins M. J. *J. Chem. Soc., Perkin Trans. 1* **1968**, 1922.
(26) Felczak, K. Unpublished results.
(27) Parr, R. G.; Yang, W. *Density-Functional Theory of Atoms and Molecules*; Oxford University Press: New York, 1989.
(28) Keresztury, G.; Jalsovszky, G. *J. Mol. Struct.* **1971**, *10*, 304.
(29) Les, A.; Adamowicz, L.; Nowak, M. J.; Lapinski, L. *Spectrochim. Acta* **1992**, *48A*, 1385.
(30) Gould, I. R.; Vincent, M. A.; Hillier, I. H.; Lapinski, L.; Nowak, M. J. *Spectrochim. Acta* **1992**, *48A*, 811.
(31) Nowak, M. J.; Lapinski, L.; Bienko, D.; Michalska, D. *Spectrochim. Acta* **1997**, *53A*, 855.
(32) Frisch, M. J.; Trucks, G. W.; Schlegel, H. B.; Gill, P. M. W.; Johnson, B. J.; Robb, M. A.; Cheeseman, J. R.; Keith, T.; Petersson; G. A.; Montgomery, J. A.; Raghavachari, K.; Al-Laham, M. A.; Zakrzewski, V. G.; Ortiz, J. V.; Foresman, J. B.; Cioslowski, J.; Stefanov, B. B.; Nanayakkara, A.; Challacombe, M.; Peng, C. Y.; Ayala, P. Y.; Chen, W.; Wong, M. W.; Andres, J. L.; Replogle, E. S.; Gomperts, R.; Martin, R. L.; Fox, D. J.; Binkley, J. S.; Defrees, D. J.; Baker, J.; Stewart, J. P.; Head-Gordon, M.; Gonzalez, C.; Pople, J. A. *Gaussian 94*, Revision D.4; Gaussian, Inc.: Pittsburgh, PA, 1995.
(33) Nowak, M. J.; Lapinski, L.; Fulara, J.; Les, A.; Adamowicz, L. *J. Phys. Chem.* **1992**, *96*, 1562.
(34) Lapinski, L.; Fulara, J.; Nowak, M. J. *Spectrochim. Acta* **1990**, *46A*, 61.
(35) Szczesniak, M.; Leszczynski, J.; Person, W. B. *J. Am. Chem. Soc.* **1992**, *114*, 2732.
(36) Stepanenko, T.; Lapinski, L.; Sobolewski A. L.; Nowak, M. J.; Kierdaszuk, B. Unpublished results.